Exact diagonalization of a one-dimensional Hubbard model at density $\rho=0.4$: Effects of Coulomb repulsions and distant transfer

F. Ouchni*
Fachbereich Physik, Universität Osnabrück, D-49069 Osnabrück, Germany

J. Schnack
Fakultät für Physik, Universität Bielefeld, Postfach 100131, D-33501 Bielefeld, Germany

J. Schulenburg
Universitätsrechenzentrum, Universität Magdeburg, D-39106 Magdeburg, Germany

(Received 10 August 2006; revised manuscript received 26 September 2007; published 2 November 2007)

An extended Hubbard model that includes not only on-site but also intersite Coulomb repulsion and distant transfer is numerically investigated using the exact Lanczos diagonalization method for finite-size systems up to $L=20$ sites. The aim is to study the charge order and unconditional dimerization of a chain at density $\rho=0.4$. From the analysis of the spin and charge correlation functions, we deduce the formation of a dimer insulating state which is a Wigner lattice-type charge ordered state. The next-nearest-neighbor hopping t_2 enhances the intradimer correlations and weakens the interdimer correlations. Implications for the CuO_2 chains in $Sr_{14}Cu_{24}O_{41}$ are discussed.

DOI: 10.1103/PhysRevB.76.195106 PACS number(s): 71.10.Fd, 71.45.Lr, 75.30.Fv

I. INTRODUCTION

Strongly anisotropic electronic systems can be modeled in terms of extended Hubbard models (EHM) which start from the tight-binding model with effective electronic repulsion that can be either short or long ranged depending on the extent of screening. The prototype of the short-range models is the one-dimensional (1D) Hubbard model which, from a mathematical point of view, can be regarded as being exactly solved for all fillings N/L, where N is the number of electrons and L the number of sites,[1] ground-state wave function, and a scheme for calculating energy and related static quantities. However, if the screening is not effective in reducing the range of the bare Coulomb repulsion, the full long-ranged or truncated (to some extent) Coulomb potential should be included. The question of importance of intersite interactions within the context of parametrized models such as EHM for low-dimensional systems was addressed by a number of authors.[2–11] Most of the studies within EHM have been done for half or quarter fillings but have not been carried out for lower densities, although many issues arise from extensive experiments on low-density systems which anticipate future investigations. The composite material $Sr_{14}Cu_{24}O_{41}$ belongs to such systems where copper and oxygen form two different substructures: CuO_2 chains and Cu_2O_3 two-leg ladders. The chains are mutually decoupled, which gives the chain subsystem its 1D nature. Each chain is a string of edge-sharing CuO_4 squares where two neighboring Cu^{2+} ions along the chain are connected via two 90° Cu–O–Cu bonds, which is a superexchange path that leads to weak ferromagnetic coupling. A copper site in cuprate materials is experimentally characterized either with a spin $S=1/2$ of the unpaired $3d^9$ electron of Cu^{2+} ion or with a hole: an effective Cu^{3+} site with $S=0$.

The spin chains in $Sr_{14}Cu_{24}O_{41}$, for which the experiments suggest that the average Cu valence in 1D chains is around +2.5, exhibit a nonmagnetic ground state with a spin gap of about 140 K and a charge order,[13] The observed spin excitations were interpreted by NMR[13] and inelastic neutron scattering[14–16] (INS) with a model in which antiferromagnetic dimers made up of next-nearest-neighbor (NNN) copper ions are weakly ferromagnetically coupled with an interdimer distance of five times the copper-copper distance ($d=5c$) as shown in Fig. 1. This configuration is consistent with 40% of the Cu ions in the magnetic Cu^{2+} state, while the remaining 60% are coupled to localized holes to form nonmagnetic Zhang-Rice singlets,[12] consistent with six holes per formula unit being located on the chains, as has been proposed by NMR.[13] This situation is shown in Fig. 1 where the charge order is of a generalized Wigner lattice (WL)-type form.[3] Hubbard has pointed out the important effect of Coulomb interactions when they are dominating the kinetic energy on the distribution of the electrons.[3] The electrons have a periodic arrangement which is a generalization of the classical WL. The ordered structure of electrons may be accompanied with a lattice distortion which is driven by electrons here. The opportunity of dimerization may be a result of competing distant transfer t_2 for NNN and Coulomb interactions. A model with t_1 [nearest-neighbor (NN) hopping] and t_2 may have some relevance to real materials such as the 1D edge-sharing chains in $Sr_{14}Cu_{24}O_{41}$. For edge-sharing chains, the largest hopping is the NNN t_2 due to the superexchange path Cu–O–O–Cu, whereas NN (Cu–Cu) hopping t_1 should be reduced due to the 90° Cu–O–Cu bond angle. In fact,

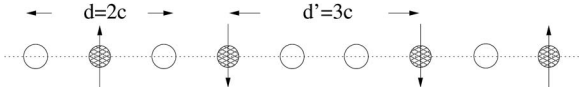

FIG. 1. Schematic representation of a model of interacting antiferromagnetic dimers along the chains of $Sr_{14}Cu_{24}O_{41}$, with lattice parameter c, suggested by INS (Refs. 14–16).

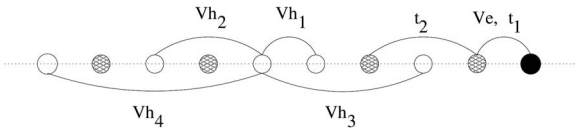

FIG. 2. Schematic representation of the single-chain EHM.

band calculations for $Sr_{14}Cu_{24}O_{41}$ show that $t_1=-0.09$ eV and $t_2=-0.17$ eV.[17]

Motivated by such experimental findings, we here investigate the ground state, as well as its charge and spin correlation functions, of an EHM at a density $\rho=0.4$. Isolated chain system is considered in this paper. Because of the complex superstructure of $Sr_{14}Cu_{24}O_{41}$, our aim is not to give a direct comparison with the experiments but rather to check whether a 1D low-density ($\rho=0.4$) system can have a WL charge ordered and dimerized ground state for some range of parameters. We hope that our results will bring some insight into the physical properties of 1D low-density systems which may motivate further investigations.

We will show that our model in its ground state has the WL charge order (CO) with dimerization and a large charge gap for large Coulomb repulsion between holes. The WL CO is stabilized by a large truncated hole-hole repulsion rather than the bare repulsion. This is realized at a specific range of the interaction which extends to the fourth neighbor. Below or above that range, the WL CO configuration competes with other configurations. The NNN hopping enhances the formation of the dimers by increasing the intradimer correlation and reducing the interdimer correlations. The short-range electron-electron (e-e) Coulomb repulsion stabilizes the dimerized state for not too large interactions.

This paper is organized as follows. In Sec. II, we introduce an EHM defined on an isolated chain (see Fig. 2). In Sec. III, we discuss our numerical results. In order to answer the above questions, we have calculated the static charge and spin structure factors as well as spin and charge gaps. Finally, in Sec. V, we summarize our results and discuss their possible experimental relevance.

II. FORMULATION OF THE MODEL

We have used an EHM with NN and NNN hoppings to consider the geometry of the edge-sharing CuO_2 chains. We have also considered the fact that the holes in these chains are localized, so bare and truncated hole-hole interactions are introduced. The WL CO suggested by Hubbard for the density $\rho=0.4$ forbids two charges to be a NN as it is shown in Fig. 1. Therefore, we have introduced a short e-e repulsion in our Hamiltonian to consider such order but also we have found that this term stabilizes the formation of the dimer singlet and enhances further the intradimer correlation function.

The model we consider is thus described by the Hamiltonian

$$H = -\sum_{i\neq j,\sigma} t_{ij} c_{i\sigma}^{\dagger} c_{j\sigma} + U\sum_{i} n_{i\uparrow} n_{i\downarrow} + \frac{1}{2}\sum_{i\neq j} Vh_{ij} n_{hi} n_{hj} + V_e \sum_{i} n_i n_{i+1}, \quad (1)$$

where $c_{i\sigma}^{\dagger}$ ($c_{i\sigma}$) is the creation (annihilation) operator of an electron with spin σ ($=\uparrow,\downarrow$) at site i and $n_{hi}=2-c_i^{\dagger}c_i$ ($n_i=c_i^{\dagger}c_i$) is the hole (electron) number operator, respectively. t_{ij} is the transfer integral; U and V_{ij} are the matrix elements of on-site and intersite Coulomb interaction, respectively (here and further on, we put $t_{i,i\pm1}=t_1$, $t_{i,i\pm2}=t_2$, and $Vh_{i,i+l}=V_h/|l|=Vh_l$, with l being the distance between holes). To distinguish between the bare and truncated Coulomb repulsion amplitudes, we put Vh_t for the bare repulsion and Vh_r for the truncated repulsion. We set $t_1=1$ and assume $U\gg t_1$, as it is the case for cuprate materials. Let us first investigate

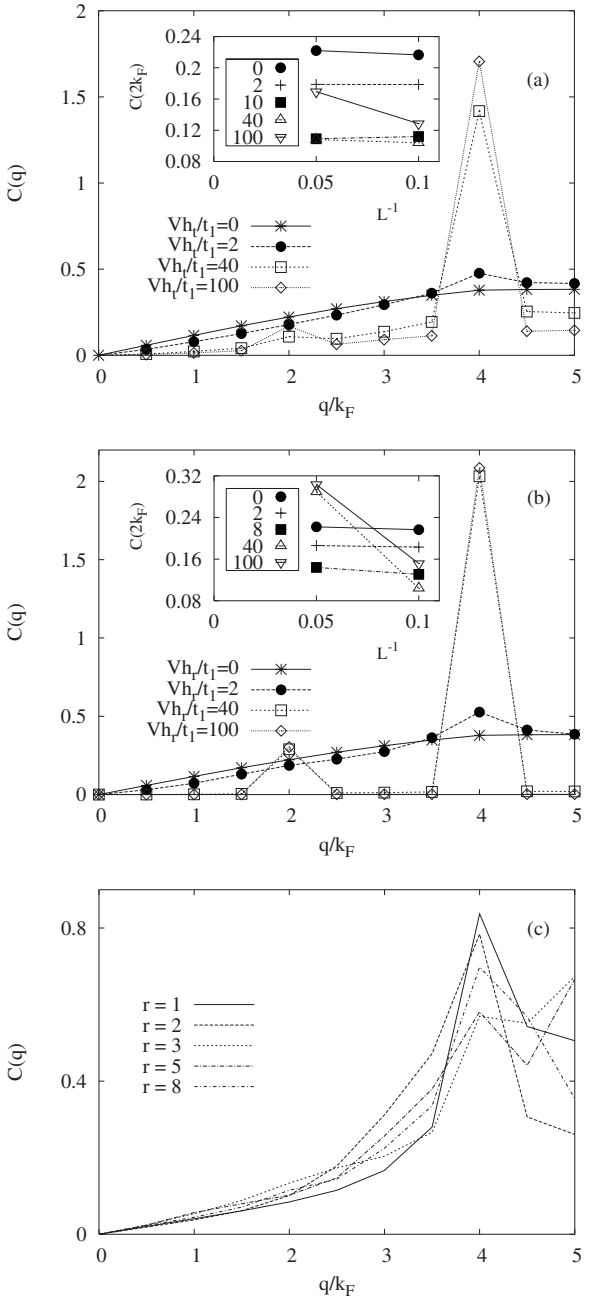

FIG. 3. Charge structure factor $C(q)$ for $L=20$. (a) and (b) at various Vh_t/t_1 (Vh_r/t_1) values, respectively. The Vh_t/t_1 and Vh_r/t_1 insets in (a) and (b), respectively, show the dependence of $C(2k_F)$ of the system size L. (c) The behavior of $C(q)$ for $r\neq 4$.

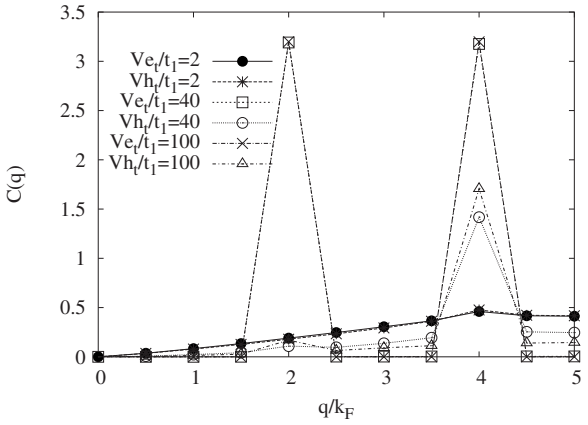

FIG. 4. $C(q)$ for $L=20$ and for both interactions: the bare hole-hole repulsion (Vh_t/t_1) and e-e repulsion (Vh_e/t_1), respectively.

the effect of Vh_l at $t_2=0$. For all calculations, we set $U=10t_1$ and treat rings with up to 20 sites.

III. RESULTS OF CALCULATION

A. Charge ordering

1. Model I

CO is a typical consequence of strong correlations, namely, large e-e Coulomb repulsion compared to the kinetic energy. This is especially due to the long-range nature of the Coulomb force. The same feature is observed here, where strong Coulomb interactions are experienced by holes. The perfect WL CO without quantum fluctuations expresses itself in the peak of the charge structure factor, which reflects the presence and nature of long-range charge correlations, shown in Fig. 3(a), and defined as

$$C(q) = \frac{1}{L}\sum_{jl} \exp(iq(j-l))(\langle n_j n_l\rangle - \langle n_j\rangle\langle n_l\rangle), \qquad (2)$$

with $n_j=n_{j\uparrow}+n_{j\downarrow}$ and $\langle n_j n_l\rangle = C((l-j)c, c=1)$ is the density-density correlation function at $q=0.4\pi$ $(=2k_F)$, which starts to increase for the bare hole-hole Coulomb repulsion with magnitude Vh_t/t_1 $(\gtrsim 40)$. Yet even at much smaller amplitudes, $C(q)$ reveals a maximum at $q=0.8\pi$ $(=4k_F)$, which indicates the persistence of pronounced short-range charge correlations. WL CO $[C(2k_F)]$ gets stronger with increasing Coulomb interaction. We note that for the model with long-range Coulomb interaction between electrons, which is well documented in the literature, the magnitude of the singularity corresponding to the periodic ordering (of WL CO types) of the charges is progressively reduced for different rational fillings.[7] At large magnitudes of the Coulomb interaction, the charge pattern obtained for the bare hole-hole Coulomb repulsion is different from that obtained using long-ranged e-e repulsion. For the same magnitude, the two interactions lead to different COs. The main CO observed for the e-e repulsion is of type

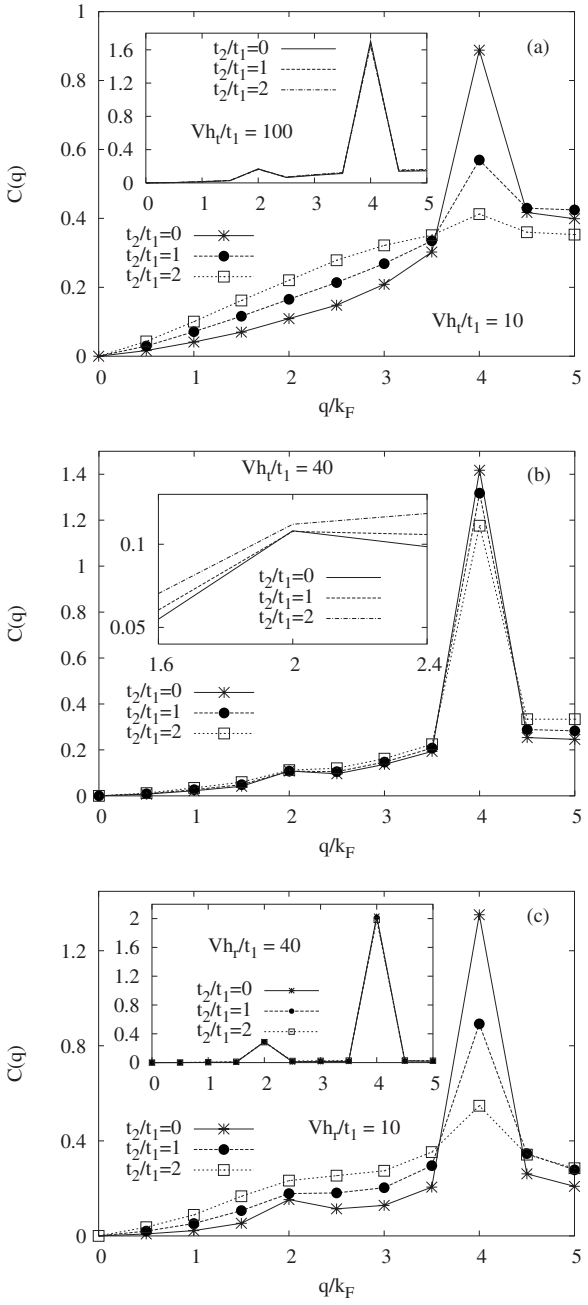

FIG. 5. Static charge structure factor $C(q)$ for $L=20$. (a) $Vh_t/t_1=10$ and different NNN hopping t_2. The inset of (a) shows the behavior of $C(q)$ for $Vh_t/t_1=40$ at various t_2 values. (b) The behavior of $C(q)$ for $Vh_t/t_1=40$ at various t_2 values. The inset shows the behavior of $C(2k_F)$ in more detail. (c) $C(q)$ for $Vh_r/t_1=10$ for different t_2. The inset of (c) shows the behavior of $C(q)$ for $Vh_r/t_1=40$ for different t_2.

0000110000110000,

where 0 represents a hole and 1 a charge. Here, the two charges 11 are on the same site and have different spins. Upon increasing Vh_t/t_1 and Ve_t/t_1, where Ve_t/t_1 is the magnitude of long-range e-e repulsion, $C(2k_F)_{Ve_t} \geqslant C(2k_F)_{Vh_t}$. However, at small magnitudes, the CO is almost the same for

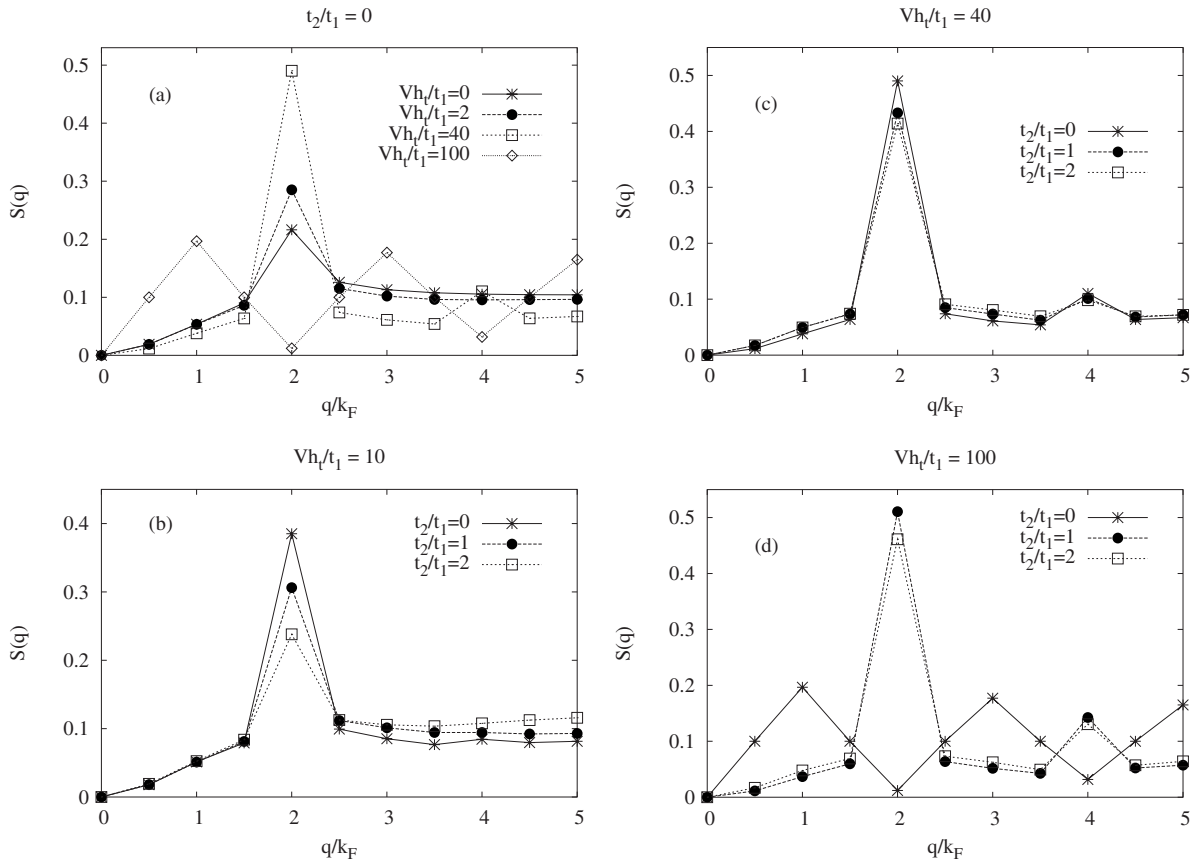

FIG. 6. Spin structure factor $S(q)$ for $L=20$ and for the bare repulsion. (a) Various Vh_t/t_1 at $t_2/t_1=0$. [(b), (c), and (d)] Different t_2 for $Vh_t/t_1=10, Vh_t/t_1=40$, and $Vh_t/t_1=100$, respectively.

both interactions, as seen in Fig. 4. Therefore, the two types of interactions lead to a different results.

The size dependence of $C(2k_F)$, shown in the inset of Fig. 3(a), suggests the $2k_F$ singularity at very large magnitudes. The same qualitative behavior of $C(q)$ holds when the Coulomb interaction, with magnitude Vh_r/t_1, is limited to some extent r. If it extends precisely to the fourth hole neighbor $r=4$, we find that the ground state of the system is dominated by configurations of WL CO type

$$\cdots 001010010100 \cdots .$$

The $C(4k_F)$ and $C(2k_F)$ peaks stabilize already at $Vh_r/t_1=40$ for Vh_r/t_1. Figure 3(b) shows how the behavior of $C(q)$ changes with varying values of Vh_r/t_1. For any $r \neq 4$ or $r \neq d_{\max}$, where $d_{\max}$ is the maximun distance between two charges and represents the bare repulsion case, WL CO configurations are absent; the $2k_F$ singularities do not show up, as seen in Fig. 3(c), which shows the behavior of $C(q)$ at $Vh_r/t_1=10$ and for different $r \neq 4$. Upon increasing r, the long-range nature of the Coulomb interactions reduces the amplitude of CO. This is in agreement with Refs. 5 and 7. Quantitatively, the $4k_F$ peaks are larger than those obtained when using the long range interaction Vh_t/t_1. The $2k_F$ peaks show up clearly already at lower Vh_r/t_1 [Vh_r/t_1 ($\gtrsim 8$)] with larger magnetudes. Thus, the truncation has a strong impact on the WL CO.

Next, we will introduce a distant hopping t_2 to investigate its effect on WL CO. We will consider mainly two cases, $t_2/t_1=1$ and $t_2/t_1=2$, to be consistent with band calculations for $Sr_{14}Cu_{24}O_{41}$ already mentioned in the Introduction.

2. Model II

The NNN hopping t_2 redistributes the charges. Upon increasing t_2/t_1 from 1 to 2, one can observe a tendency to create a homogeneous distribution of the charges. In the parameter ranges $40 < Vh_t/t_1 < 100$ and $Vh_r/t_1 < 20$, the $2k_F$ peaks disappear [see Figs. 5(a) and 5(c)]. Thus, large t_2 weakens CO and helps destabilize it for not too large magnitudes of interactions which are needed to compensate the effect of t_2.

B. Spin correlations

1. Model I

In order to study the spin degrees of freedom of the system, we now calculate the static spin structure factor $S(q)$, the Fourier transform of spin-spin correlation function $\langle S_i^z S_{i+l}^z \rangle$, with $S_i^z=(n_{i\uparrow}-n_{i\downarrow})/2$, shown in Figs. 6(a) and 7(b), defined as

$$S(q) = \frac{1}{L} \sum_{il} \langle S_i^Z S_{i+l}^Z \rangle e^{iql}. \quad (3)$$

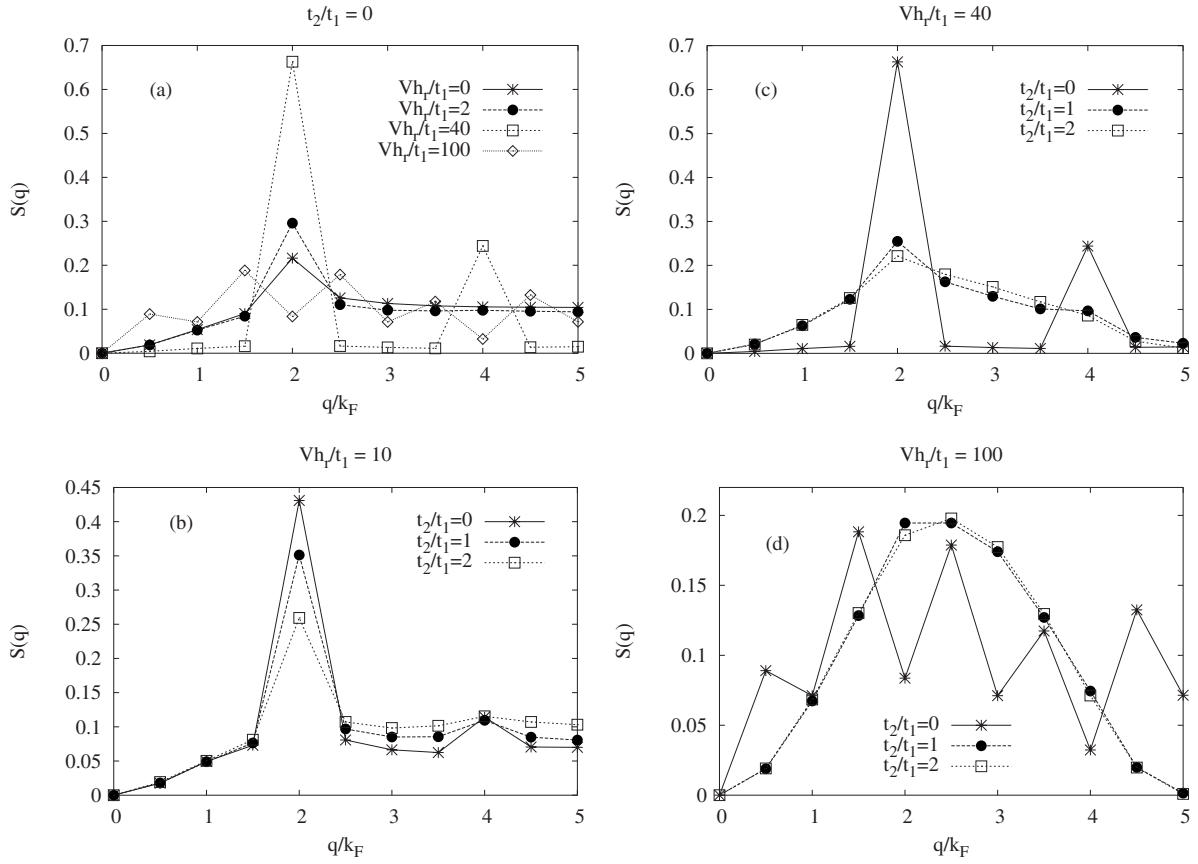

FIG. 7. Spin structure factor $S(q)$ for $L=20$ and for the truncated repulsion for $r=4$. (a) Various Vh_r/t_1 at $t_2/t_1=0$. [(b), (c), and (d)] Different t_2 for $Vh_r/t_1=10, Vh_r/t_1=40$, and $Vh_r/t_1=100$, respectively.

$S(q)$ displays two peaks: a large and dominant peak at $2k_F$ and a smaller peak at $4k_F$. The peak at $2k_F$, which is 0.2 in units of the reciprocal lattice vector, was also observed by INS.[15,16] The $2k_F$ peaks saturate at $40<Vh_t/t_1<100$ $(Vh_r/t_1=40)$ and are suppressed at $Vh_t/t_1(Vh_r/t_1)=100$. This result is due to the fact that configurations with different spin structures for NNN charges and for charges separated by the distance d, where d is the distance representing the WL CO periodicity, have a large weight in the ground state. For instance, $\downarrow 0\uparrow$, $\downarrow 0\downarrow$, and $\uparrow 0\uparrow$ as spin structures for NNN charges and $\uparrow 0\uparrow 00\downarrow$, $\uparrow 0\downarrow 00\uparrow$,…, as spin structures for charges separated by d. The behavior of the singularity corresponding here to the WL CO is different from that observed for e-e repulsion in Ref. 7, where the magnitude of the singularity corresponding to the periodic ordering of the charges is progressively reduced, for different rational fillings, upon increasing the magnitude of the repulsion. Therefore, the two types of interaction lead again to a different result. Indeed, Fig. 8 shows our calculation of $S(q)$, which now has a different singularity $(q=\pi)$ as those observed for long-range hole-hole interaction $(q=2k_F,4k_F)$. Upon increasing Ve_t/t_1, the magnitude of $S(q)$ at the singularity $q=\pi$ is reduced, which is consistent with Ref. 7. The $4k_F$ peaks are absent when the interactions are turned off and suppressed at $Vh_t/t_1(Vh_r/t_1)=100$. We do not have a well defined spin structure for NNN charges. The ground state has no dimer structure. In what follows, we will show the important role of a NNN hopping t_2 on spin configurations.

2. Model II

For the model of interacting antiferromagnetic dimers, proposed by INS and shown in Fig. 1, the dominant interaction is the intradimer interaction which is much larger than the interdimer interactions. Our results for fixed t_2/t_1 show that both Coulomb interactions decrease distant spin-spin correlation function $S(l)$, defined by $S(l)=\langle S_i S_{i+l}\rangle$, shown in

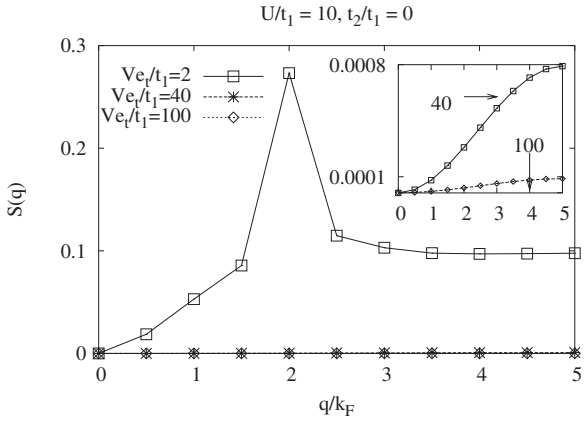

FIG. 8. Spin structure factor $S(q)$ for the long-range e-e repulsion Ve_t/t_1 for $L=20$ at $t_2/t_1=0$. The inset shows in more detail the behavior of $S(q)$ for $L=20$ at $Ve_t/t_1=40$ and $Ve_t/t_1=100$, respectively.

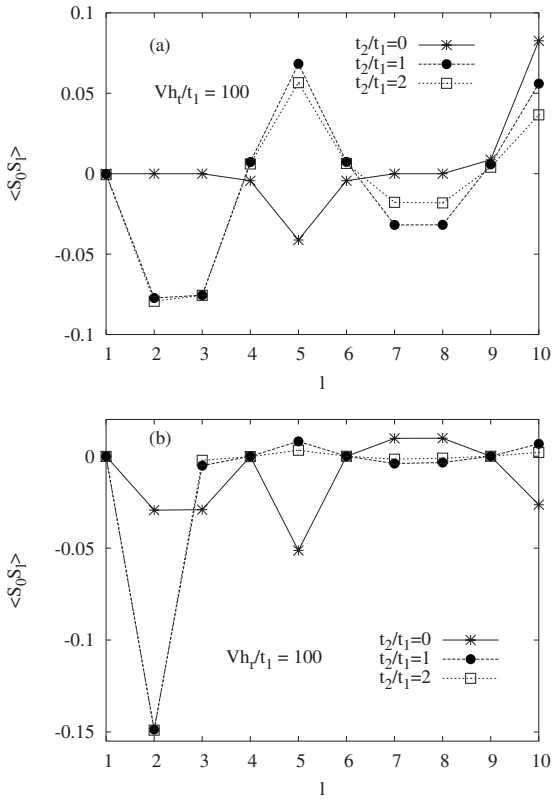

FIG. 9. Spin-spin correlation function $\langle S_0 S_l \rangle$ for $L=20$ at various t_2/t_1 values. (a) The bare repulsion of magnitude $Vh_t/t_1=100$. (b) The truncated repulsion of magnitude $Vh_r/t_1=100$.

Figs. 9(a) and 9(b). The decrease is larger for Vh_r/t_1. Upon increasing t_2/t_1, $S(l)$ decreases further. An interesting result is obtained at $Vh_r/t_1=100$ where distant correlations become negligible and the dominated correlation is $S(2)$, whereas for the same value for Vh_t/t_1, $S(3)$ and $S(5)$ are still of almost the same magnitude as $S(2)$. Thus, the effect of t_2 on spin configurations for the bare Coulomb repulsion is less relevant to obtain a dimerized ground state than for the truncated interaction. Therefore, we have obtained the WL CO state with dominated intradimer and week interdimer correlations $(S(2)/|S(5)|=27.92)$ for very large Vh_r/t_1 and NNN hopping t_2. However, in our model, the WL CO configuration with the spin structure suggested by INS competes with configurations having other spin structures as it is shown below,

$$00\uparrow 0\downarrow 00\uparrow 0\downarrow 00\uparrow 0\downarrow 00\downarrow 0\uparrow,$$

$$00\uparrow 0\downarrow 00\uparrow 0\downarrow 00\downarrow 0\uparrow 00\downarrow 0\uparrow,$$

$$00\uparrow 0\downarrow 00\uparrow 0\downarrow 00\uparrow 0\downarrow 00\uparrow 0\downarrow,$$

$$00\uparrow 0\downarrow 00\downarrow 0\uparrow 00\uparrow 0\downarrow 00\downarrow 0\uparrow.$$

$S(q)$ is plotted in Figs. 6 and 7. $S(2k_F)$ and $S(4k_F)$ are t_2/t_1 dependent. $S(2k_F)$ decreases under the effect of t_2, whereas $S(4k_F)$ stays unchanged for $Vh_t/t_1 \leqslant 40$. For $Vh_r/t_1=100$, $S(q)$ becomes smooth, and the singularity assigned at $2k_F$ has

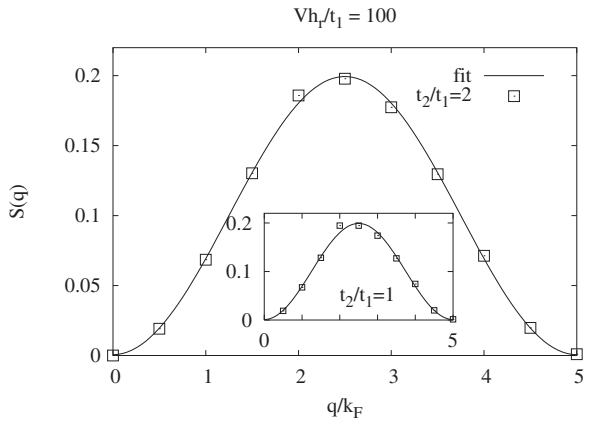

FIG. 10. Spin structure factor $S(q)$ for $L=20$ and $Vh_r/t_1=100$ for $t_2/t_1=2$. The inset represents $S(q)$ for $t_2/t_1=1$. The full line in both plots represents a fit to an isolated dimers made up by two NNN spins.

shifted to $2.5k_F$ and the $4k_F$ peaks are suppressed. This is in accord with Matsuda *et al.*,[18] who observed in INS measurements a maximum of the intensity around 0.25 in units of the reciprocal lattice vector. If the main contribution to $S(q)$ comes from $\langle S_i^z S_{i+2}^z \rangle$ then, from Eq. (3), $S(q)$ can be approximated by $S(q) \sim \langle S_i^z S_i^z \rangle + 2\langle S_i^z S_{i+2}^z \rangle \cos(2q)$. Therefore, we have fitted $S(q)$ by a function like $F(q)=A+B\cos(2q)$ shown in Fig. 10. Table I shows the parameters A, B, $\langle S_i^z S_i^z \rangle$, and $\langle S_i^z S_{i+2}^z \rangle$.

3. Effect of V_e

The short e-e repulsion $V_e \neq 10$ has an effect for not too large Vh_r/t_1 values $(Vh_r/t_1 \leqslant 40)$. It stabilizes the dimer formation as it is shown in Fig. 11. It enhances $S(2k_F)$ but does not change its position. The behavior at small momenta remains the same, and for $q > 2k_F$, the decrease becomes a bit slower for large V_e/t_1 values. However, for $V_e/t_1=10(V_e=U)$, there is a shift of the maximum to $2.5k_F$. Thus, our results show that at $\rho=0.4$, models with large values of Vh_r/t_1, together with NNN hopping t_2, and models with intermediate values of Vh_r/t_1 and NN e-e repulsion V_e lead to a shift of the $2k_F$ peaks to $2.5k_F$. The $2.5k_F$ singularity is observed by INS[18] and can be obtained within a model in which a lattice distortion with four times the periodicity of the chain structure is required, provided by NMR,[13] for the case where one hole is transferred to a ladder, i.e., half-filled chains.

The next step is to check the behavior of the charge and spin gaps and critical exponent. We will consider only the

TABLE I. The parameters A and B obtained from the fit for $Vh_r/t_1=100$ and different t_2/t_1 ratios. For each t_2/t_1, one can observe that $A \sim \langle S_i^z S_i^z \rangle$ and $B \sim \langle S_i^z S_{i+2}^z \rangle$.

	A	B	$\langle S_i^z S_i^z \rangle$	$\langle S_i^z S_{i+2}^z \rangle$
$t_2/t_1=1$	0.0999745	−0.049699	0.099997	−0.049586
$t_2/t_1=2$	0.1000709	−0.0495118	0.099986	−0.049688

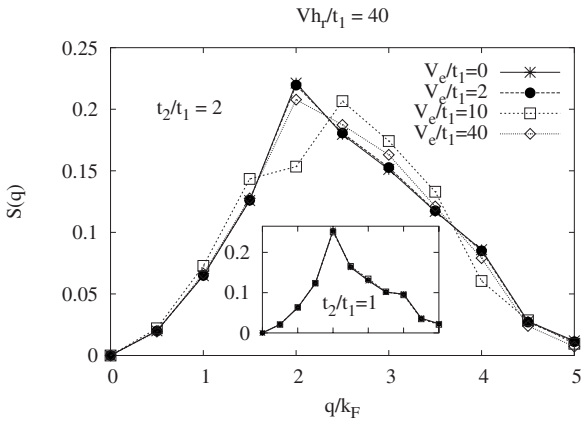

FIG. 11. Static spin structure factor $S(q)$ for $L=20$ and $Vh_r/t_1=40, t_2/t_1=2$, and various V_e/t_1. The inset shows the behavior of $S(q)$ for $t_2/t_1=1$ and various V_e/t_1. Clearly, V_e has no effect on $S(q)$ for $t_2/t_1=1$.

truncated repulsion, as it reproduces better the results for WL CO and dimerization. Thus, we will restrict the calculation using model II for intermediate and large Vh_r/t_1 values. Due to the restriction to the density $\rho=0.4$, we can produce simulation data for three sizes only $(L=10,15,20)$. In order to avoid even-odd fluctuations, we will consider only two sizes $(L=10,20)$. Therefore, our estimates for infinite chains have to be understood as rough approximations. It might be possible to advance to bigger systems using density matrix renormalization group (DMRG) techniques, but this is left for future investigations.

C. Charge gap

The charge gap is given by

$$\Delta_c(N;L) = E_0(N+1;L) + E_0(N-1;L) - 2E_0(N;L), \quad (4)$$

where $E_0(M;L)$ denotes the ground-state energy of a M particles on L sites. Our results for $\Delta_c(L)$ are shown in Figs. 12(a) and 12(b) for $10 \leqslant Vh_r/t_1 \leqslant 100$, together with the extrapolation to the large N limit. A linear fit (LF) $A+B/L$ leads to an unphysical negative value in case of $Vh_r/t_1=10$ and $t_2/t_1=2$, which might be due to the uncertainties of the finite-size scaling. Such an effect is absent with a quadratic fit (QF) $A+B/L^2$. $\Delta_c(L)$ increases with increasing Vh_r/t_1 in the considered parameters range. It is small at $Vh_r/t_1=10$ but stays finite for large system denoted by lines which represent the extrapolation to the thermodynamic limit. The full line corresponds to a linear fit and the dashed line to a quadratic fit. At large Coulomb repulsion, a charge gap clearly opens up. Thus, the insulating region is confined to large values of Vh_r/t_1. The NNN hopping t_2 decreases Δ_c by a small amount.

D. Spin gap

The spin gap may be defined by

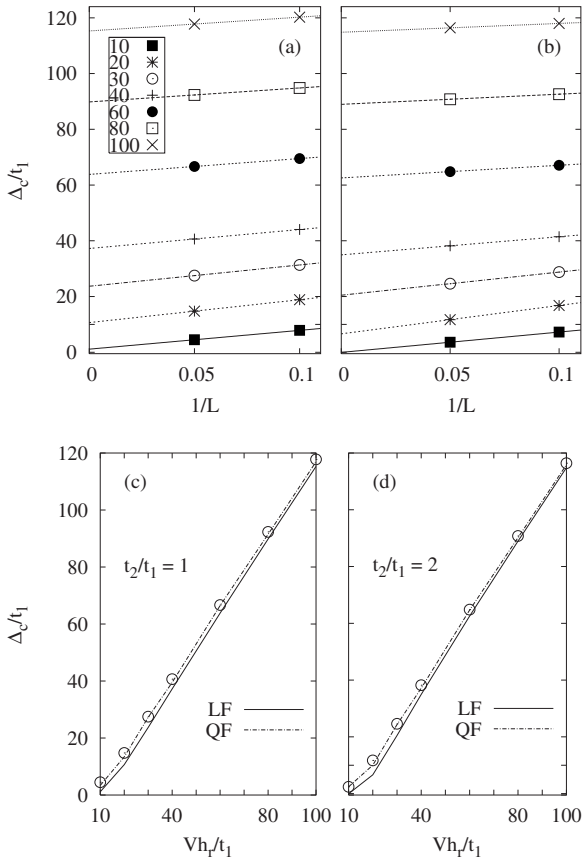

FIG. 12. Charge gap $\Delta_c(L)$ as defined in Eq. (4). (a) and (b) show the dependence of $\Delta_c(L)$ of the system size L for $t_2/t_1=1$ and $t_2/t_1=2$, respectively, for different Vh_r/t_1 values. [(c) and (d)] $\Delta_c(L)$ for $L=20$ and large Vh_r/t_1 values: (c) $t_2/t_1=1$ and (d) $t_2/t_1=2$. The full and dashed lines represent LF and QF, respectively, to large limit.

$$\Delta_s(N;L) = E_0(N_\uparrow+1;N_\downarrow-1;L) - E_0(N_\uparrow;N_\downarrow;L). \quad (5)$$

It corresponds to the energy needed to make a triplet excitation from the singlet ground state. Generally, the spin gap is much smaller than the charge gap, which is the case here. So, an accurate calculation is required. However, with the sizes that are available, it is not possible to distinguish any spin structure that will remain in the thermodynamic limit with a good accuracy. Other numerical techniques such as DMRG are required. The calculated results for $\Delta_s(L)$ as a function of Vh_r/t_1 and t_2/t_1 are shown in Figs. 13(a) and 13(b). Δ_s fluctuates strongly with the number of sites. $\Delta_s(L=10)=0$ for any Vh_r/t_1 and the ground state is degenerate, while $\Delta_s(L=20)$ changes by varying Vh_r/t_1 in the parameter range shown in Fig. 13(b). One may observe the same qualitative behavior of $\Delta_s(L)$ for $t_2/t_1=1$ and $t_2/t_1=2$, whereas the maximum $\Delta_s^c(L)$ for $t_2/t_1=2$ is much larger than that for $t_2/t_1=1$ by an amount of 5.8 $[\Delta_s^c(t_2/t_1=2)\sim 0.094, \Delta_s^c(t_2/t_1=1)\sim 0.016]$. For fixed t_2/t_1, $\Delta_s(L=20)$ is almost zero at $Vh_r/t_1=10$ and increases to reach a maximum for a given magnitude Vh_r^c/t_1. The position and the magnitude of the maximum $\Delta_s^c(L)$ depend on the ratio t_2/t_1. For $t_2/t_1=1$,

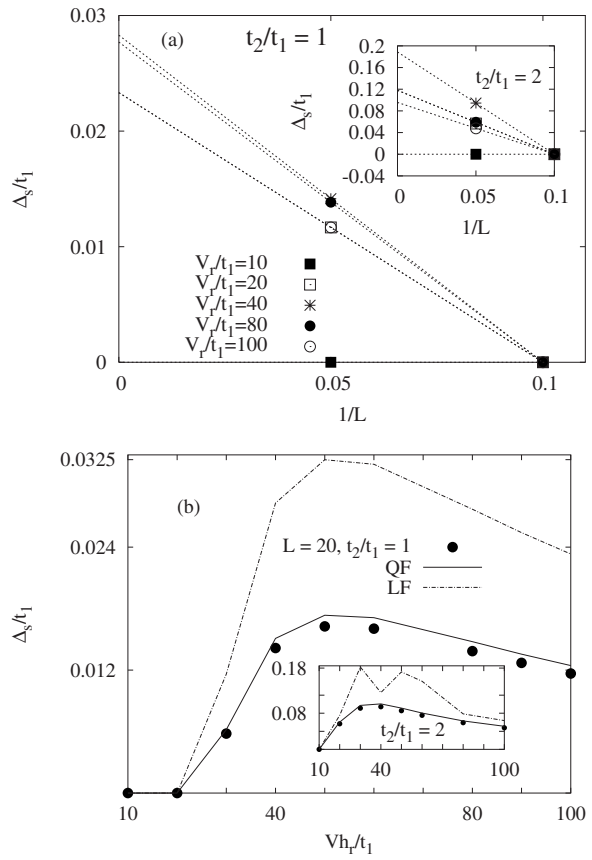

FIG. 13. Spin gap $\Delta_s(L)$ as defined in Eq. (5). (a) The dependence of $\Delta_s(L)$ of the system size L for $t_2/t_1=1$ and $t_2/t_1=2$, respectively, for different Vh_r/t_1 values. (b) $\Delta_s(L)$ for $L=20$ and large Vh_r/t_1 values: (c) $t_2/t_1=1$ and (d) $t_2/t_1=2$. The full line represents the fit to large limit. The dotted line in the inset is guide to the eye.

$Vh_r^c/t_1=50$. While for $t_2/t_1=2$, $Vh_r^c/t_1=40$. On the other hand, the spin gap observed for the 1D chain in $Sr_{14}Cu_{24}O_{41}$ is about $\Delta_s^{exp}\sim 140$ K, which corresponds to $0.12t_1$ (assuming $t_1\sim 0.1$ eV to be consistent with band calculations[17]). Our numerical results show that the finite-size spin gap for $Vh_r/t_1=40$, $V_{ee}/t_1=10$, and $t_2/t_1=1$ is about $\Delta_s\sim 0.124t_1$. Also, for larger magnitudes, when V_{ee} is not considered, $\Delta_s^c(L)\sim 0.127t_1$ for $Vh_r/t_1=90$ at $t_2/t_1=1$, while the result for the large L limit obtained for $Vh_r/t_1=100$ by the quadratic fit gives a value about $\sim 0.124t_1$. The linear fit gives larger values than Δ_s^{exp}. So, from these finite-size results and their quadratic extrapolation to large L limit, a gapped spectrum may be obtained at larger magnitudes $(Vh_r/t_1>10)$ where the system contains singlet pairs as seen from the behavior of the spin-spin correlation functions. A close finite-size results to Δ_s^{exp} can be obtained within our model II for $t_2/t_1=1$ at $Vh_r/t_1=40$ and $V_e=10t_1$, or for $80<Vh_r/t_1<90$. If the QF reflects the true large L limit, then a close value to Δ_s^{exp} can be obtained for $90<Vh_r/t_1<100$. Thus, more calculations should be performed to get more accurate results for Δ_s.

IV. SUMMARY AND DISCUSSION

We have studied the spin and charge correlations of a chain by means of an extended Hubbard model using exact diagonalization. At a density of $\rho=0.4$, the properties of such a model are not known so far. We have shown that the model generates CO of WL at large Coulomb repulsion between holes. This WL CO is stabilized by the truncated interaction to the fourth neighbor. The formation of dimers is a result of the competition between the Coulomb repulsion and distant transfer. This later enhances largely $S(2)$, the spin-spin correlation between NNN charges forming the dimer, and weakens the distant interdimer correlations. When hole-hole Coulomb repulsion is not too large, a short e-e repulsion is needed to stabilize the dimer formation. We have also found that the system shows an insulating behavior for intermediate and large interactions through the behavior of the charge gap. However, a possible finite spin gap can be obtained only for very large interaction.

ACKNOWLEDGMENTS

We would like to thank Thierry Giamarchi, Satoshi Ejima, Belen Valenzuela, and Mohamed Azzouz for helpful discussions of this work and related topics and for accepting to read the paper.

*fouchni@uos.de

[1] E. H. Lieb and F. Y. Wu, Phys. Rev. Lett. **20**, 1445 (1968).
[2] J. Kondo and K. Yamai, J. Phys. Soc. Jpn. **43**, 424 (1977).
[3] J. Hubbard, Phys. Rev. B **17**, 494 (1978).
[4] L. Arrachea and A. A. Aligia, Phys. Rev. Lett. **73**, 2240 (1994).
[5] S. Capponi, D. Poilblanc, and T. Giamarchi, Phys. Rev. B **61**, 13410 (2000).
[6] Hitoshi Seo and Masao Ogata, Phys. Rev. B **64**, 113103 (2001).
[7] B. Valenzuela, S. Fratini, and D. Baeriswyl, Phys. Rev. B **68**, 045112 (2003).
[8] M. Daghofer and P. Horsch, Phys. Rev. B **75**, 125116 (2007).
[9] S. Nishimoto and Y. Ohta, Phys. Rev. B **68**, 235114 (2003).
[10] P. Horsch, M. Sofin, M. Mayr, and M. Jansen, Phys. Rev. Lett. **94**, 076403 (2005).
[11] Matthias Mayr and Peter Horsch, Phys. Rev. B **73**, 195103 (2006).
[12] F. C. Zhang and T. M. Rice, Phys. Rev. B **37**, 3759 (1988).
[13] M. Takigawa, N. Motoyama, H. Eisaki, and S. Uchida, Phys. Rev. B **57**, 1124 (1998).
[14] U. Ammerahl, B. Buchner, L. Colonescu, R. Gross, and A. Revcolevschi, Phys. Rev. B **62**, 8630 (2000).
[15] L. P. Regnault, J. P. Boucher, H. Moudden, J. E. Lorenzo, A. Hiess, U. Ammerahl, G. Dhalenne, and A. Revcolevschi, Phys. Rev. B **59**, 1055 (1999).
[16] R. S. Eccleston, M. Uehara, J. Akimitsu, H. Eisaki, N. Motoyama, and S. I. Uchida, Phys. Rev. Lett. **81**, 1702 (1998).
[17] M. Arai, and H. Tsunetsugu, Phys. Rev. B **56**, R4305 (1997).
[18] M. Matsuda, K. Katsumata, H. Eisaki, N. Motoyama, S. Uchida, S. M. Shapiro, and G. Shirane, Phys. Rev. B **54**, 12199 (1996).